Contribution from the Laboratoire de Chimie Inorganique, URA CNRS 420, Institut de Chimie Moléculaire, Université Paris-Sud, 91405 Orsay, France, Service National des Champs Intenses CNRS, 38042 Grenoble, France, and Departamento de Cristalografia, Mineralogia y Depositos Minerales, Universidad de Barcelona, Barcelona 08007, Spain

Structure of the Linear Trinuclear Complex $Mn^{II}_3(CH_3CO_2)_6(bpy)_2$. Determination of the *J* Electron-Exchange Parameter through Magnetic Susceptibility and High-Field Magnetization Measurements

S. Ménage,[†] S. E. Vitols,[†,‡] P. Bergerat,[†] E. Codjovi,[†] O. Kahn,[*,†] J.-J. Girerd,[*,†] M. Guillot,[§] X. Solans,[∥] and T. Calvet[∥]

Received May 8, 1990

The new trinuclear cluster $Mn^{II}_3(CH_3CO_2)_6(bpy)_2$ has been synthesized, and its crystal structure was determined. It crystallizes in the triclinic system, space group $P\bar{1}$, with a = 12.849 (4) Å, b = 9.790 (3) Å, c = 8.187 (2) Å, α = 108.50 (2)°, β = 96.69 (2)°, γ = 106.41 (3)°, Z = 1, and V = 912.5 (5) Å^3. The structure was solved and refined by using 2071 reflections with $I \geq 2.5\sigma(I)$ collected in the range 2° $\leq \theta \leq$ 25°. Final values of conventional indices R and R_w were 5.1% and 4.8%, respectively. The structure consists of linear trinuclear molecules; each pair of manganese atoms are bridged by three acetato groups, two of them acting as bidentate bridges and a third one bridging by one oxygen atom only. The central manganese has a coordination sphere made of six oxygen atoms from six different acetato groups, and the terminal ones have a distorted environment of four oxygen atoms and two nitrogen atoms that come from a bipyridine molecule. The molar magnetic susceptibility χ_M has been investigated as a function of temperature T. The $\chi_M T$ product is equal to 11.87 cm^3 mol^{-1} K at 285 K and decreases to 4.32 cm^3 mol^{-1} K at 4.2 K. The data have been fitted with an expression for the magnetic susceptibility derived from the Van Vleck formula by using the solutions of the spin Hamiltonian $H = -J(\mathbf{S}_1\cdot\mathbf{S}_2 + \mathbf{S}_2\cdot\mathbf{S}_3) - J_{13}\mathbf{S}_1\cdot\mathbf{S}_3$. Taking $J_{13} = 0$, we found $J = -4.4$ cm^{-1}. The ground state was found to be the $|S_2 = {}^5/_2, S_{13} = 5, S = {}^5/_2\rangle$ state. Confirmation of the nature of the ground state and the energy ordering of the lowest excited states was obtained by measuring the magnetization as a function of the magnetic field up to 20 T at 4.2 K. The crossover between the $|S_2 = {}^5/_2, S_{13} = 5, S = {}^5/_2\rangle$ and the $|S_2 = {}^5/_2, S_{13} = 5, S = {}^7/_2\rangle$ states was observed. Those measurements constitute an independent determination of the J exchange parameter: the J value was found to be in perfect agreement with the one deduced from magnetic susceptibility measurements. A preliminary EPR study at room and helium temperatures is reported.

Introduction

The chemistry of manganese polynuclear complexes has received a strong impulse from the rapidly growing biochemistry of this element, in particular from the study of the role of a still mysterious manganese cluster in oxygen evolution by plants.[1,2] Recently several reviews on manganese chemistry appeared.[3-6] In particular, ref 6 is devoted to the very rich chemistry of manganese with the carboxylate anion.

The system manganese-acetate-bipyridine has given several well-characterized compounds. Christou et al. have reported[7] the structure of two tetranuclear complexes: $[Mn^{III}_4O_2(CH_3CO_2)_7(bpy)_2]^+$ and $Mn^{III}_2Mn^{II}_2O_2(CH_3CO_2)_6(bpy)_2$. We reported[8] the structure of the dinuclear unit $[Mn^{III}_2O(CH_3CO_2)_2(bpy)_2(H_2O)_2]^{2+}$, which was the first of this type with a bidentate terminal ligand; similar complexes have been prepared with tridentate terminal ligands: $[Mn^{III}_2O(CH_3CO_2)_2L'_2]^{2+}$,[9] where L' is 1,4,7-trimethyl-1,4,7-triazacyclononane, and $Mn^{III}_2O(CH_3CO_2)_2(HB(pz)_3)_2$,[10] where $HB(pz)_3^-$ is the tripyrazolborato anion, but in those cases there is no free position for the substrate coordination. Manganese-acetate-bipyridine chemistry has been recently enriched by the preparation of $Mn^{III}Mn^{IV}O_2(CH_3CO_2)Cl_2(bpy)_2$[11] and $Mn^{III}_2O(CH_3CO_2)_2(bpy)_2Cl_2$.[6]

We present here the synthesis, crystal structure, and magnetic properties of the new linear trinuclear complex $Mn^{II}_3(CH_3CO_2)_6(bpy)_2$. The benzoato analogue has been obtained and its crystal structure published by Christou.[6] An analogous $Fe^{II}_3(CH_3CO_2)_6(bpy)_2$ complex has been characterized by Lippard et al.[12]

Trinuclear complexes offer the opportunity to test the Heisenberg model on more complicated systems[13] than the extensively studied dinuclear systems. We will discuss the reliability of magnetic susceptibility measurements to determine the energy of the spin states for this trinuclear cluster. A confirmation of the validity of this approach was obtained through high-field (20 T) magnetization measurements at 4.2 K. This is one of the rare determinations of the J exchange coupling parameter by this technique.[14]

As far as bioinorganic chemistry is concerned, several trinuclear systems have drawn attention. A linear $[Fe_3S_4]^+$ unit[15] and triangular $[Fe_3S_4]^{n+}$ sites (n = 1;[16] n = 0[17]) have been studied. A trinuclear Cu site has been characterized by X-ray diffraction in ascorbate oxidase.[18] Recently a mononuclear plus trinuclear arrangement has been proposed for manganese atoms of the oxygen evolving complex in plants.[19,20] A trinuclear species

[†] Université Paris-Sud.
[‡] Present address: Department of Chemistry, Princeton University, Princeton, NJ 08542.
[§] Service National des Champs Intenses CNRS.
[∥] Universidad de Barcelona.

(1) Brudvig, G. W.; Beck, W. F.; de Paula, J. C. *Annu. Rev. Biophys. Chem.* **1989**, *18*, 25-46.
(2) Rutherford, A. W. *Trends Biochem. Sci.* **1989**, *14*, 227-232.
(3) Pecoraro, V. L. *Photochem. Photobiol.* **1988**, *48*, 249-264.
(4) Vincent, J. B.; Christou, G. *Adv. Inorg. Chem.* **1989**, *33*, 197-257.
(5) Wieghardt, K. *Angew. Chem., Int. Ed. Engl.* **1989**, *28*, 1153-1172.
(6) Christou, G. *Acc. Chem. Res.* **1989**, *22*, 328-335.
(7) Vincent, J. B.; Christmas, C.; Chang, H.-R.; Li, Q.; Boyd, P. D. W.; Huffman, J. C.; Hendrickson, D. N.; Christou, G. *J. Am. Chem. Soc.* **1989**, *111*, 2086-2097.
(8) Ménage, S.; Girerd, J.-J.; Gleizes, A. J. *Chem. Soc., Chem. Commun.* **1988**, 431-432.
(9) (a) Wieghardt, K.; Bossek, U.; Ventur, D.; Weiss, J. *J. Chem. Soc., Chem. Commun.* **1985**, 347. (b) Wieghardt, K.; Bossek, K.; Nuber, B.; Weiss, J.; Bonvoisin, J.; Corbella, M.; Vitols, S. E.; Girerd, J.-J. *J. Am. Chem. Soc.* **1988**, *110*, 7398-7411.
(10) Sheats, J. E.; Czernuszewicz, R. S.; Dismukes, G. C.; Rheingold, A. L.; Petrouleas, V.; Stubbe, J.; Armstrong, W. H.; Beer, R. H.; Lippard, S. J. *J. Am. Chem. soc.* **1987**, *109*, 1435-1444.
(11) Bashkin, J. S.; Schake, A. R.; Vincent, J. B.; Chang, H.-R.; Li, Q.; Huffman, J. C.; Christou, G.; Hendrickson, D. N. *J. Chem. Soc., Chem. Commun.* **1988**, 700-702.
(12) Rardin, R. L.; Bino, A.; Poganiuch, P.; Tolman, W. B.; Liu, S.; Lippard, S. J. *Angew. Chem., Int. Ed. Engl.* **1990**, *29*, 812-814.
(13) Kahn, O. Magnetism of Heteropolymetallic Systems. *Struct. Bonding* **1987**, *68*, 89-167.
(14) Qiang, X.; Darriet, J. *C. R. Acad. Sci. Paris* **1986**, *303*, 1637-1639.
(15) Girerd, J.-J.; Papaefthymiou, G. C.; Watson, A. D.; Gamp, E.; Hagen, K. S.; Edelstein, N.; Frankel, R. B.; Holm, R. H. *J. Am. Chem. Soc.* **1984**, *106*, 5941-5947.
(16) Kent, T. A.; Huynh, B. H.; Munck, E. *Proc. Natl. Acad. Sci. U.S.A.* **1980**, *77*, 6574-6576.
(17) Papaefthymiou, V.; Girerd, J.-J.; Moura, I. Moura, J. J. G.; Munck, E. *J. Am. Chem. Soc.* **1987**, *109*, 4703-4710.
(18) Messerschmidt, A.; Rossi, A.; Ladenstein, R.; Huber, R.; Bolognesi, M.; Gatti, G.; Marchesini, A.; Petruzzelli, R.; Finazziagro, A. *J. Mol. Biol.* **1989**, *206*.

Table I. Summary of Crystallographic Data for $Mn_3(CH_3CO_2)_6(bpy)_2$

formula	$C_{32}H_{34}Mn_3N_4O_{12}$	β, deg	96.69 (2)
fw	831.46	γ, deg	106.41 (3)
radiation, Å	0.71069	V, Å^3	912.5 (5)
temp, K	288	Z	1
space group	$P\bar{1}$	d_{calcd}, g/cm^3	1.513
a, Å	12.849 (4)	μ, cm^{-1}	11.41
b, Å	9.790 (3)	$R(F_0^2)$	0.051
c, Å	8.817 (2)	$R_w(F_0^2)$	0.048
α, deg	108.50 (2)		

$Mn^{II}Mn^{III}_2(SALADHP)_2(CH_3CO_2)_4(CH_3OH)_2$ has been studied in detail.[21] We recently characterized a $[Mn_3O_4]^{4+}$ core.[22]

Finally, we will note that the bridging scheme in $Mn^{II}_3(CH_3CO_2)_6(bpy)_2$ is close to the one found in $Mn(CH_3CO_2)_2 \cdot 4H_2O$, which is also made of linear trinuclear units and has been much studied as an example of a 2D ferromagnetic lattice (see ref 23). The magnetic properties of those two compounds will be compared.

Experimental Section

Synthesis. Synthesis was carried out under argon. $Mn(CH_3CO_2)_2 \cdot 4H_2O$ (245 mg, 1 mmol) was dissolved in 10 mL of degassed pure EtOH. A 10-mL solution of bpy (156 mg, 1 mmol) in EtOH was transferred to the first one. After 10 min of stirring, the resulting yellow solution was partially evaporated, giving the desired product as a yellow crystalline powder in excellent yield (≈70% based on Mn). The powder was washed with cold ethanol under argon. Crystals can be obtained by slow evaporation under argon of an ethanol solution. Anal. Calcd for $C_{32}H_{34}Mn_3N_4O_{12}$: C, 46.23; H, 4.12; N, 6.74; Mn, 19.82. Found: C, 46.83; H, 3.87; N, 6.17; Mn, 18.84.

Magnetic Susceptibility Measurements. Magnetic susceptibility measurements in the 3–300 K temperature range were carried out with a Faraday-type magnetometer equipped with a helium continuous-flow cryostat. Automatic data-acquisition equipment was made at the Laboratoire de Chimie Inorganique. $HgCo(NCS)_4$ was used as a susceptibility standard.

High-Field Magnetization Measurements. The molar magnetization M was measured as a function of the magnetic field up to 20 T at 4.2 K by means of a fluxmetric method. The sample, directly immersed in the liquid-helium bath, was extracted in a constant magnetic field between compensated pick-up coils connected in series opposition, and the integrated signal was proportionnal to M. The calibration and the sensitivity of the apparatus were previously described in detail.[24]

Crystallographic Data Collections and Refinement of the Structure. A prismatic crystal (0.1 × 0.1 × 0.15 mm) was selected and mounted on a Philips PW-1100 four-circle diffractometer. Information concerning conditions for crystallographic data collection and structure refinement is summarized in Table I. Unit-cell parameters were determined from 25 reflections ($4 \leq \theta \leq 12°$) and refined by least-squares methods. A total of 2247 reflections were measured in the range $2 \leq \theta \leq 25°$, 2071 of which were assumed as observed by applying the condition $I \geq 2.5\sigma(I)$. Three reflections were measured every 2 h as orientation and intensity control; significant intensity decay was not observed. Lorentz-polarization but no absorption corrections were made. The structure was solved by direct methods, using the MULTAN system of computer programs,[25] and refined by full-matrix least-squares methods, using the SHELX76 program.[26] The positions of 17 H atoms were located from a difference synthesis and refined with an overall isotropic thermal parameter, and the remaining atoms were refined anisotropically. The final R was 0.051 for all observed reflections. The atomic coordinates for the non-hydrogen atoms are given in Table II: those for the hydrogen atoms are given in Table S1. The main bond lengths and angles are given in Table III.

EPR Spectra. These were recorded on powder samples at X-band frequency with a Bruker ER 200D spectrometer equipped with an helium

(19) Penner-Hahn, J. E.; Fronko, R. M.; Pecoraro, V. L.; Yocum, C. F.; Betts, S. C.; Bowlby, N. R. *J. Am. Chem. Soc.* **1990**, *112*, 2549–2557.
(20) George, G. N.; Prince, R. C.; Cramer, S. P. *Science* **1989**, *243*, 789.
(21) Li, X.; Kessissoglou, D. P.; Kirk, M. L.; Bender, C. J.; Pecoraro, V. L. *Inorg. Chem.* **1988**, *27*, 1–3.
(22) Auger, N.; Girerd, J.-J.; Corbella, M.; Gleizes, A.; Zimmermann, J.-L. *J. Am. Chem. soc.* **1990**, *112*, 448–450.
(23) Carlin, R. L. *Magnetochemistry*; Springer-Verlag: Berlin, 1986.
(24) Picoche, J.; Guillot, M.; Marchand, A. *Physica* **1989**, *B155*, 407–410.
(25) Main, P.; Fiske, S. E.; Hull, S. L.; Lessinger, L.; Germain, G.; Declercq, J. P.; Woolfson, M. M. MULTAN, an automatic system of computer programs for crystal structure determination from X-ray diffraction data. University of York, England, University of Louvain, Belgium, 1984.
(26) Sheldrick, G. M. SHELX. A computer program for crystal structure determination. Univ. of Cambridge, England, 1976.

Table II. Final Atomic Coordinates (×10⁴) of $Mn_3(CH_3CO_2)_6(bpy)_2$

	x/a	y/b	z/c
Mn(1)	2311 (1)	3509 (1)	1977 (1)
Mn(2)	5000 (0)	5000 (0)	5000 (0)
N(1)	432 (4)	2447 (5)	975 (6)
C(1)	−232 (5)	1561 (8)	1666 (10)
C(2)	−1363 (6)	898 (8)	999 (10)
C(3)	−1830 (5)	1175 (9)	−402 (11)
C(4)	−1165 (5)	2106 (8)	−1112 (9)
C(5)	−28 (4)	2719 (6)	−401 (8)
C(6)	762 (5)	3678 (6)	−1127 (7)
C(7)	421 (5)	4081 (8)	−2530 (9)
C(8)	1217 (6)	4930 (9)	−3148 (9)
C(9)	2312 (6)	5343 (8)	−2398 (10)
C(10)	2590 (5)	4898 (8)	−1026 (9)
N(10)	1847 (4)	4101 (5)	−365 (6)
O(11)	3785 (3)	3138 (5)	5408 (6)
C(11)	2779 (5)	2335 (7)	4919 (8)
O(12)	2091 (3)	2373 (5)	3719 (6)
C(12)	2310 (8)	1233 (11)	5767 (12)
O(13)	5018 (3)	3473 (5)	2426 (6)
C(13)	4351 (5)	2645 (7)	975 (8)
O(14)	3340 (3)	2474 (5)	608 (5)
C(14)	4773 (8)	1766 (12)	−501 (12)
O(15)	3669 (3)	5541 (4)	3665 (5)
C(15)	3210 (5)	6561 (7)	4087 (8)
O(16)	2193 (4)	6192 (6)	3651 (6)
C(16)	3923 (8)	8177 (11)	5051 (16)

Table III. Selected Bond Lengths (Å) and Angles (deg) for $Mn_3(CH_3CO_2)_6(bpy)_2$

Around Mn(1)			
Mn(1)–O(12)	2.067 (4)	N(10)–Mn(1)–N(1)	72.2 (2)
Mn(1)–O(14)	2.101 (4)	O(12)–Mn(1)–N(1)	85.3 (2)
Mn(1)–O(15)	2.155 (4)	O(12)–Mn(1)–O(15)	98.8 (2)
Mn(1)–O(16)	2.605 (5)	O(15)–Mn(1)–N(10)	102.6 (2)
Mn(1)–N(1)	2.272 (4)	O(14)–Mn(1)–N(10)	87.6 (2)
Mn(1)–N(10)	2.236 (5)	O(14)–Mn(1)–O(12)	99.3 (2)
		O(15)–Mn(1)–O(14)	94.2 (2)
		O(16)–Mn(1)–N(1)	92.3 (2)
		O(16)–Mn(1)–N(10)	81.5 (2)
		O(16)–Mn(1)–O(12)	105.0 (2)
		O(15)–Mn(1)–O(16)	53.1 (1)
Mn(1)–Mn(2)	3.614 (1)		
Around Mn(2)			
Mn(2)–O(11)	2.185 (4)	O(13)–Mn(2)–O(11)	91.3 (2)
Mn(2)–O(13)	2.170 (4)	O(15)–Mn(2)–O(11)	91.5 (1)
Mn(2)–O(15)	2.200 (4)	O(15)–Mn(2)–O(13)	88.0 (2)
Bridge			
Mn(1)–Mn(2)	3.614 (1)	Mn(1)–O(15)–Mn(2)	112.2
Acetate Groups			
O(16)–C(15)	1.228 (7)	O(16)–C(15)–O(15)	119.7 (6)
O(15)–C(15)	1.276 (7)		
O(13)–C(13)	1.249 (7)	O(14)–C(13)–O(13)	126.0 (6)
O(14)–C(13)	1.250 (7)		
O(12)–C(11)	1.260 (7)	O(11)–C(11)–O(12)	124.7 (6)
O(11)–C(11)	1.246 (7)		

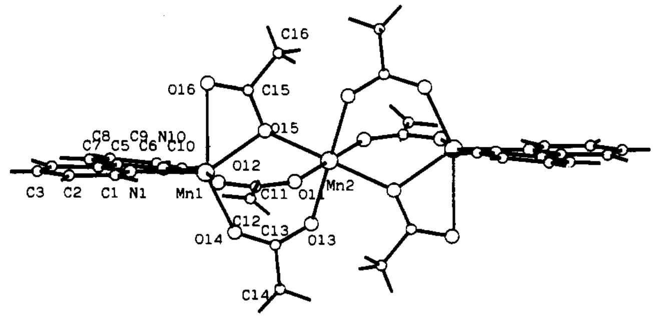

Figure 1. Perspective view of $Mn_3(CH_3CO_2)_6(bpy)_2$.

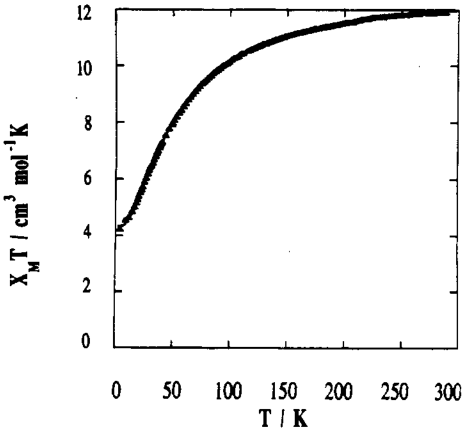

Figure 2. $\chi_M T$ versus T plot for $Mn_3(CH_3CO_2)_6(bpy)_2$: (▲) experimental points; (–) calculated curve.

continuous-flow cryostat. The magnetic field was determined with a Hall probe, and the klystron frequency, with a Hewlett-Packard frequency meter.

Results

Structure of $Mn_3(CH_3CO_2)_6(bpy)_2$. The structure is represented in Figure 1. It consists of trinuclear units of Mn atoms, where each pair of manganese atoms are μ-linked by three acetate ligands. Two of the acetate groups are bridging as bidentate ligands and the third one is bridging through one oxygen atom only; this third acetato group chelates the terminal manganese atom. The molecule has an inversion center, which is a crystallographic symmetry. Mn(2) is on the inversion center and displays an octahedral coordination, being linked to six O atoms of six acetate ligands, while the Mn(1) is linked to two N atoms of a bipyridine ligand. The acute N(1)–Mn(1)–N(10) (72.2 (2)°) and O(15)–Mn(1)–O(16) (53.1 (1)°) bond angles produce significant differences in the coordination sphere with respect to regular octahedral coordination. Around Mn(1), the Mn–O distances are shorter than the Mn–N ones except for the distance Mn(1)–O(16) = 2.605 Å, which is the largest one (see Discussion). The Mn(1)···Mn(2) separation is equal to 3.614 (1) Å.

Magnetic Susceptibility Measurements. We measured the molar magnetic susceptibility χ_M of $Mn_3(CH_3CO_2)_6(bpy)_2$ as a function of the temperature T. The results are shown in Figure 2 in the form of the $\chi_M T$ versus T plot. $\chi_M T$ decreases from 11.87 cm^3 mol^{-1} K at 285 K to 4.32 cm^3 mol^{-1} K at 4.2 K. The room-temperature $\chi_M T$ value is smaller than the expected value $\chi_M T = (N\beta^2/3k)3g_i^2S_i(S_i + 1) = 13.125$ cm^3 mol^{-1} K for three Mn(II) atoms uncoupled with $S_i = {}^5/_2$ and $g_i = 2$ each. This is already indicative of substantial antiferromagnetic coupling. It is confirmed by the dramatic decrease of $\chi_M T$ when T decreases. At low temperature, the value of $\chi_M T$ corresponds (within experimental uncertainty) to the expected value $\chi_M T = (N\beta^2/3k)g^2S(S + 1) = 4.375$ cm^3 mol^{-1} K for a spin $S = {}^5/_2$ state with $g = 2$.

Taking into account the structure of this compound, we used the following Heisenberg Hamiltonian to describe the low-lying electronic states

$$H_S = -J(\mathbf{S}_1\cdot\mathbf{S}_2 + \mathbf{S}_2\cdot\mathbf{S}_3) - J_{13}\mathbf{S}_1\cdot\mathbf{S}_3$$

where $\mathbf{S}_i$ is the spin of the Mn ion number i in Figure 1. The eigenvalues are given by

$$E(S_{13},S) = -(J/2)[S(S + 1) - S_{13}(S_{13} + 1)] - (J_{13}/2)S_{13}(S_{13} + 1)$$

where S is the total spin of the molecular and S_{13} is the spin quantum number associated with the spin $\mathbf{S}_{13} = \mathbf{S}_1 + \mathbf{S}_3$ of the terminal Mn ions. We have the conditions $0 \le S_{13} \le 5$ and $|S_{13} - {}^5/_2| \le S \le S_{13} + {}^5/_2$. The possible values for S and S_{13} are given in Table IV together with the energy of each spin state for the case $J_{13} = 0$.

We added to the preceding Hamiltonian the Zeeman term

$$H_{Zeeman} = \textstyle\sum_i g_i \beta S_{iz} H$$

Table IV. Values of the Total Spin S, of the Subspin S_{13}, and of the Energy of Each $|S_{13},S\rangle$ State in Units of J for $J_{13} = 0$[a]

S	S_{13}	$E(S_{13},S)/-J$	S	S_{13}	$E(S_{13},S)/-J$
$^{15}/_2$	5	27.5	$^5/_2$	5	0
$^{13}/_2$	5	20.0		4	5
	4	25.0		3	9
$^{11}/_2$	5	13.5		2	12.0
	4	18.5		1	14.0
	3	22.5		0	15.0
$^9/_2$	5	8.0	$^3/_2$	4	2.5
	4	13.0		3	6.5
	3	17.0		2	9.5
	2	20.0		1	11.5
$^7/_2$	5	3.5	$^1/_2$	3	5
	4	8.5		2	8
	3	12.5			
	2	15.5			
	1	17.5			

[a] The energy of the ground state $|S_{13} = 5, S = {}^5/_2\rangle$ is taken as the energy origin.

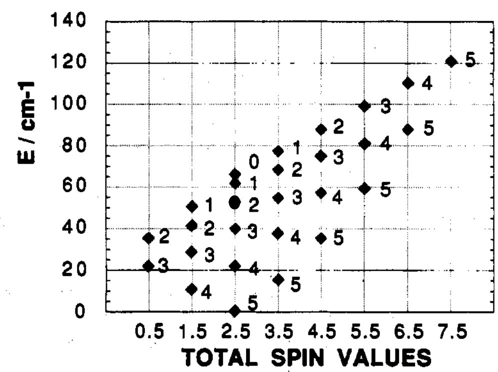

Figure 3. Spin levels for $Mn_3(CH_3CO_2)_6(bpy)_2$ with $J = -4.4$ cm^{-1}. The energy in cm^{-1} is given as a function of the spin value. To the right of the levels, the S_{13} values are given.

where g_i for individual Mn(II) ions were considered isotropic and $g_i = g$, so that H_{Zeeman} simplifies considerably to $H_{Zeeman} = g\beta S_z H$. The Van Vleck expression for the susceptibility is then

$$\chi_M = \frac{Ng^2\beta^2}{3kT}\,\frac{\sum_{S_{13},S} S(S + 1)(2S + 1)\exp\left[-\dfrac{E(S_{13},S)}{kT}\right]}{\sum_{S_{13},S}(2S + 1)\exp\left[-\dfrac{E(S_{13},S)}{kT}\right]}$$

From the structure, we are allowed to think that $|J_{13}/J| \ll 1$. For instance, in $Mn_3Br_{12}^{6-}$, this ratio was found by neutron diffraction to be equal to 0.014.[27] So we fixed $J_{13} = 0$. The best fit was obtained for $J = -4.4$ cm^{-1} and $g = 1.99$. The agreement between this calculation and experimental data is excellent as can be judged from Figure 2. The agreement factor defined as $R = \sum([\chi_M T]^{exp} - [\chi_M T]_{calc})^2/([\chi_M T]^{exp})^2$ is $R = 2 \times 10^{-5}$. Energy levels are represented in Figure 3 in the way introduced in ref 28. We add here the S_{13} label. The ground state is found to be the $|S_2 = {}^5/_2, S_{13} = 5, S = {}^5/_2\rangle$ state, the first excited state is the quartet state $|S_2 = {}^5/_2, S_{13} = 4, S = {}^3/_2\rangle$ at 11 cm^{-1}, and then the $|S_2 = {}^5/_2, S_{13} = 5, S = {}^7/_2\rangle$ state occurs at 15.4 cm^{-1}; all the states are indicated in Figure 3. At room temperature, all the states are populated.

High-Field-Magnetization Study. Taking into account the antiferromagnetic character and the relative weakness of the magnetic interaction between Mn(II) ions, we have explored an alternative method to determine J, namely the study of the magnetization up to very high field. The magnetization M versus

(27) Falk, U.; Furrer, A.; Furer, N.; Gudel, H. U.; Kjems, J. K. *Phys. Rev. B* **1987**, *35*, 4893–4900.
(28) Pei, Y.; Journaux, Y.; Kahn, O. *Inorg. Chem.* **1988**, *27*, 399–404.

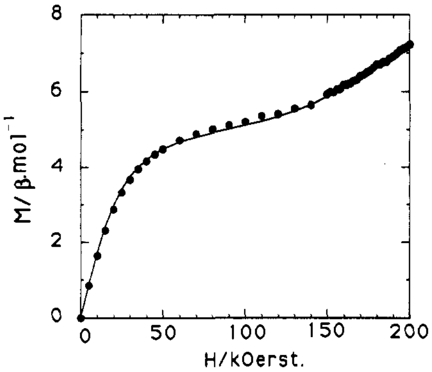

Figure 4. Molar magnetization M in μ_B versus field H in kOe.

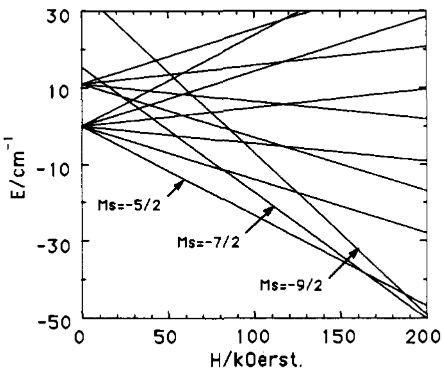

Figure 5. Energy (in cm^{-1}) of the lowest levels as a function of magnetic field with H in kOe. Note the spin crossover at very high field.

H curve at 4.2 K, reported in Figure 4, is, up to 10 T, close to a Brillouin function with $S = {}^5/_2$. This was expected for a spin sextet ground state. But, instead of showing a saturation magnetization $M_{sat} = g({}^5/_2\beta)$ above 10 T, M continuously increases and reaches 7.2β at 20 T. This behavior may be explained as follows: at 4.2 K and at low field, the different components of the $|S_2 = {}^5/_2, S_{13} = 5, S = {}^5/_2\rangle$ state and not much of the other states, are populated. When H increases, the role of the Zeeman term becomes preponderant. In particular, the gaps between the ground state $|S_2 = {}^5/_2, S_{13} = 5, S = {}^5/_2, M_S = -{}^5/_2\rangle$ and the spin states $|S_2, S_{13}, S, M_S\rangle$, where $M_S < -{}^5/_2$, decrease. The variations of the low-lying state energies versus the field are reported in Figure 5. This diagram emphasizes the stabilization of both the $|S_2 = {}^5/_2, S_{13} = 5, S = {}^7/_2, M_S = -{}^7/_2\rangle$ and $|S_2 = {}^5/_2, S_{13} = 5, S = {}^9/_2, M_S = -{}^9/_2\rangle$ levels in a 20-T field. Those levels intersect the $|S_2 = {}^5/_2, S_{13} = 5, S = {}^5/_2, M_S = -{}^5/_2\rangle$ level at $H_1 = 7J/2g\beta$ (around 16.2 T) and $H_2 = 4J/g\beta$ (around 18.9 T). The magnetization rise is due to the thermal population of the $|S_2 = {}^5/_2, S_{13} = 5, S = {}^7_2, M_S = -{}^7/_2\rangle$ and $|S_2 = {}^5/_2, S_{13} = 5, S = {}^9/_2, M_S = -{}^9/_2\rangle$ levels. The other levels with lower $|M_S|$ values are not significantly stabilized at 20 T. To fit the magnetization curve, we are allowed to consider that, at 4.2 K and in the 0–20-T field range, the populated spin states are $|S_2 = {}^5/_2, S_{13} = 5, S = {}^5/_2, M_S\rangle$, $|S_2 = {}^5/_2, S_{13} = 4, S = {}^3/_2, M_S\rangle$, $|S_2 = {}^5/_2, S_{13} = 5, S = {}^7/_2, M_S = -{}^7/_2\rangle$, and $|S_2 = {}^5/_2, S_{13} = 5, S = {}^9/_2, M_S = -{}^9/_2\rangle$. The same assumptions as in the susceptibility fitting ($J_{13}/J \ll 1$ and $g_i = g$ isotropic) lead to the following expression of the molecular magnetization

$$M = (Ng\beta/2)\,(\mathrm{d}Z/\mathrm{d}x)/Z$$

where Z is the partition function

$$Z = [\cosh(5x) + \cosh(3x) + \cosh(x)] + [\cosh(3x) + \cosh(x)]\exp(-3y/2) + \exp(7x - 7y/2) + \exp(9x - 8y)$$

with $x = g\beta H/kT$ and $y = J/kT$.

The best fit was obtained for $J = -4.4$ cm^{-1} and $g = 1.985$ in very good agreement with both values deduced from the magnetic susceptibility data.

EPR Spectra. At 300 K, the EPR spectrum (Figure 7a) is very broad (more than 4200 G). At 10 K, fine structure is resolved (Figure 7b), and a complicated spectrum is observed with resonances at $g = 6.3$, 3.0, 2.05, 1.7, and 1.04. At room temperature, many spin levels are occupied since $J = -4.4$ cm^{-1}; the broadness of the spectrum suggests that ZFS is not negligible: when the ZFS is negligible for systems with $|J| > |A|$ (A is the hyperfine splitting parameter), a narrow spectrum is observed around $g = 2$, as explained in ref 29. Such a narrow spectrum has been observed in ref 30. The importance of ZFS is confirmed in the 10 K spectrum where fine structure is observed. A quantitative explanation of this low-temperature spectrum is being studied.

Discussion

The ease of synthesis of this trinuclear complex proves the ability of the manganese–carboxylate–bpy system to form polynuclear complexes and makes this compound a good candidate for physical studies.

$Mn^{II}_3(CH_3CO_2)_6(bpy)_2$ contains a new example of the $Mn_2(RCO_2)_2(OR)^{n+}$ core. Such a unit has been observed with $Mn^{IV}Mn^{III}$, $Mn^{III}Mn^{III}$, $Mn^{III}Mn^{II}$, and $Mn^{II}Mn^{II}$ oxidation states as reviewed in refs 3–6. Our compound is the analogue of the benzoate trinuclear complex $Mn^{II}_3(PhCO_2)_6(bpy)_2$ first reported in ref 6.

The structure of those $Mn^{II}_3(RCO_2)_6(bpy)_2$ compounds are clearly related to the structure of $Mn(CH_3CO_2)_2{\cdot}4H_2O$, which is also made of trinuclear units,[31] in which the Mn–Mn distance is 3.6 Å, identical with the one found in $Mn_3(RCO_2)_6(bpy)_2$ (see this work and ref 6). In $Mn(CH_3CO_2)_2{\cdot}4H_2O$, the terminal Mn atoms are much closer to octahedral geometry than in our compound. The carboxylate bridging the Mn atoms by one oxygen atom in $Mn(CH_3CO_2)_2{\cdot}4H_2O$ links, through the second oxygen atom, a trinuclear unit to another one in such a way that those trinuclear units form planes. The planes are separated from each other by 9.6 Å giving to the compound a pronounced 2-D character. In the bpy complex, the analogous acetato group is chelating so that the trinuclear units are independent from each other.

The duality in the type of bridging modes of acetate groups, bidentate or monodentate bridging, is remarkable. It has been recently observed for formate anions in $Fe_2(HCO_2)_4(BIPhMe)_2$[32,33] and for acetate ones in $Fe_3(CH_3CO_2)_6(bpy)_2$.[12] One characteristic of the monodentate bridging acetate is that it leads to a weak bond between Mn(1) and O(16) atoms (Mn(1)–O(16) distance = 2.605 Å). Note that the O–C–O angle of this acetate group (119.7°) is more acute than the same angle (126° or 124.7°) for the other acetate groups, which is due to this Mn(1)–O(16) interaction. The same features were observed in $Fe_2(HCO_2)_4(BIPhMe)_2$[32,33] and in $Fe_3(CH_3CO_2)_6(bpy)_2$ although less pronounced: in the former one the Fe–O long distance is 2.787 Å and in the latter one, the distance of the analogous bond is 3.005 Å.[33]

From a magnetic point of view, our system has a $|S_2 = {}^5/_2, S_{13} = 5, S = {}^5/_2\rangle$ ground state, which can be depicted simply as

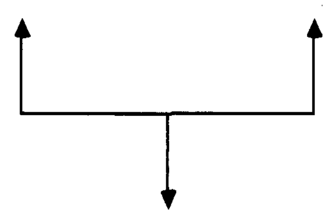

The lowest energy levels can be identified in Figure 3. The first excited state is $|S_2 = {}^5/_2, S_{13} = 4, S = {}^3/_2\rangle$ at $2.5|J| = 11.0$ cm^{-1}. Then we find $|S_2 = {}^5/_2, S_{13} = 5, S = {}^7/_2\rangle$ at $3.5|J| = 15.4$ cm^{-1}.

(29) Ishikawa, Y. *J. Phys. Soc. Jpn.* **1966**, *12*, 1473–1481.
(30) Luneau, D.; Savariault, J. M.; Tuchagues, J. P. *Inorg. Chem.* **1988**, *27*, 3912–3918.
(31) Bertaut, E. F.; Duc, T. Q.; Burlet, P.; Thomas, M.; Moreau, J. M. *Acta Crystallogr.* **1974**, *B30*, 2234–2236.
(32) Tolman, W. B.; Bino, A.; Lippard, S. J. *J. Am. Chem. Soc.* **1989**, 111, 8522–8523.
(33) Tolman, W. B.; Liu, S.; Bentsen, J. G.; Lippard, S. J. *J. Am. Chem. Soc.* **1991**, *113*, 152–164.

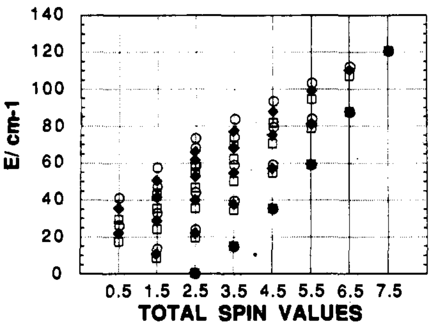

Figure 6. Spin levels for $Mn_3(CH_3CO_2)_6(bpy)_2$ with $J = -4.4\ cm^{-1}$: (○) $J_{13} = +0.5\ cm^{-1}$; (□) $J_{13} = -0.5\ cm^{-1}$; (◆) $J_{13} = 0$.

To what degree can we be sure of the values of the energies deduced from magnetic susceptibility measurements and reproduced in Figure 3? We do not know the value of J_{13} but we know from the large distance between Mn(1) and Mn(3) atoms and from analogous experiments on $Mn_3Br_{12}^{6-}$ that $|J_{13}/J| \ll 1$. The real diagram must not be very different from Figure 3.

From fitting trials (not shown), we found that $|J_{13}|$ is at most equal to 0.5 cm^{-1}: greater values induce detectable variations in the curve $\chi_M = f(T)$. Figure 6 gives the energy of the spin states for $J = -4.4\ cm^{-1}$ and for $J_{13} = -0.5$, 0, and +0.5 cm^{-1}. First, one can note that the states with the same S_{13} value as the one of the ground state ($S_{13} = 5$) are separated from the ground state by gaps independent of J_{13} (which is evident from the expression for the energy). The other states are affected by J_{13}, but the perturbation is greater for those states that differ greatly from the ground state in their S_{13} value. In particular the $S_{13} = 4$ states are not very much affected. At most (i.e. for $|S_2 = {}^5/_2, S_{13} = 0, S = {}^5/_2\rangle$) the deviation is about 10%, which is quite acceptable. In conclusion, the use of magnetic susceptibility data is a good method to deduce the spin-state scheme of systems in which all the spin states are populated at high temperature and become differentially populated at low temperature.

A spectacular demonstration is brought to fruition through the use of high-field magnetization measurements. Using very high field (20 T), we were able to observe the cross over of the $|S_2 = {}^5/_2, S_{13} = 5, S = {}^5/_2, M_S = -{}^5/_2\rangle$ and the $|S_2 = {}^5/_2, S_{13} = 5, S = {}^7/_2, M_S = -{}^7/_2\rangle$ states, which gives a direct access to the separation between those states in the zero field and thus to J. The value of J so obtained was in perfect agreement with the value obtained from magnetic susceptibility measurement. A very high magnetic field can break the antiferromagnetic coupling inside the trinuclear unit; this behavior toward H is analogous to the metamagnetism in weakly coupled antiferromagnetic materials. To the best of our knowledge, such an approach has been used only once (for a molecular divanadyl entity).[14]

Note that it was impossible to deduce J_{13} from this technique. The magnetization curve is in fact essentially sensitive to the relative energies of the ground state and the higher spin multiplicity states; the gaps between $|S_2 = {}^5/_2, S_{13} = 5, S = {}^5/_2, M_S = -{}^5/_2\rangle$,$|S_2 = {}^5/_2, S_{13} = 5, S = {}^7/_2, M_S = -{}^7/_2\rangle$ and $|S_2 = {}^5/_2, S_{13} = 5, S = {}^9/_2, M_S = -{}^9/_2\rangle$ are unrelated to J_{13} since the three levels have the same S_{13} value.

The magnetization curves are often influenced by the anisotropy. The magnetization study at lower temperatures might provide information on the anisotropic parameters as a detailed EPR study.

Magnetic properties of $Mn(CH_3CO_2)_2 \cdot 4H_2O$ have been studied and were explained (see ref 23) as issuing from antiferromagentically coupled trinuclear units, ferromagnetically coupled together in planes. In turn, the planes are antiferromagnetically coupled. The antiferromagnetic intracluster interaction has been considered as the leading one. Saturation magnetization studies (see ref 23) gave one spin $S = {}^5/_2$ per three manganese atoms. Our results on $Mn_3(CH_3CO_2)_6(bpy)_2$ confirm that the intracluster interaction is antiferromagnetic and such that at low temperatures only one $S = {}^5/_2$ remains for three manganese atoms.

Trinuclear $Mn_3Br_{12}^{6-}$ units obtained in $CsMn_xMg_{1-x}Br_3$ have been studied in ref 27 by inelastic neutron scattering, which

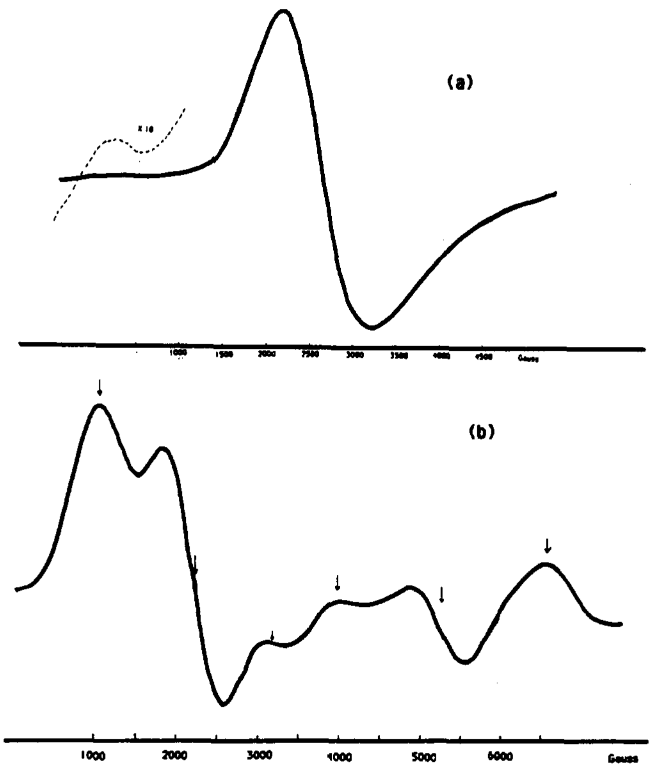

Figure 7. EPR spectra of $Mn_3(CH_3CO_2)_6(bpy)_2$ (a) at 200 K and (b) at 10 K.

allowed determination of the second nearest-neighbor coupling constant; the ratio J_{13}/J was found equal to 1.4%. The spin state energy pattern found for this system is very close to the one we found for our system.

Another resported linear manganese trinuclear complex is $Mn^{II}Mn^{III}_2(SALADHP)_2(CH_3CO_2)_4(CH_3OH)_2$, the bridge structure of which is very close to that of our compound.[21] In this case, a $|S_2 = {}^5/_2, S_{13} = 4, S = {}^3/_2\rangle$ ground state has been observed as expected from a simple scheme analogous to the one above.

The J value found in $Mn^{II}_3(CH_3CO_2)_6(bpy)_2$ can be compared with other $Mn^{II}Mn^{II}$ magnetic interactions implying acetato groups. It is slightly larger than the $J = -3.5\ cm^{-1}$ we found[9b] for $[L'_2Mn_2(CH_3CO_2)_3]^+$ but much smaller than the value measured for $[L'_2Mn_2(CH_3CO_2)_2OH]^+$ ($J = -18\ cm^{-1}$; L' is 1,4,7-trimethyl-1,4,7-triazacyclononane).[34] The weakest interaction in $[L'_2Mn_2(CH_3CO_2)_3]^+$ could be related to the larger Mn–Mn distance (4.034 Å) observed in this compound versus the 3.6-Å distance observed in $Mn^{II}_3(CH_3CO_2)_6(bpy)_2$. A better reason could be that the monoatomic oxygen bridge in $Mn^{II}_3(CH_3CO_2)_6(bpy)_2$ is more efficient for electron exchange than the triatomic acetato bridge in $[L'_2Mn_2(CH_3CO_2)_3]^+$.

Finally, the large difference in J values between $Mn^{II}_3(CH_3CO_2)_6(bpy)_2$ and $[L'_2Mn_2(CH_3CO_2)_2OH]^+$ is striking. The $[Mn_2(CH_3CO_2)_2(OR)]^+$ unit with a hydroxo bridge (R = H) presents a much stronger J coupling than the analogous complex with a monodentate acetato bridge ($R = CH_3CO$). The same effect occurs in analogous Fe(II) complexes: in $Fe_2(HCO_2)_4(BIPhMe)_2$ the J is found to be practically equal to zero in contrast with the $J = -26\ cm^{-1}$ value in $[L'_2Fe_2(CH_3CO_2)_2OH]^+$.[35] Lippard et al. have recently related this phenomenon to larger Fe–O(bridging) distances in $Fe_2(HCO_2)_4(BIPhMe)_2$ than in $[L'_2Fe_2(CH_3CO_2)_2OH]^+$.[33] The same explanation seems to be valid here: in $[L'_2Mn_2(CH_3CO_2)_2OH]^+$ the geometry of the

(34) Wieghardt, K.; Bossek, U.; Bonvoisin, J.; Beauvillain, P.; Girerd, J.-J.; Nuber, B.; Weiss, J.; Heinze, J. *Angew. Chem., Int. Ed. Engl.* **1986**, *25*, 1030–1031.
(35) Hartman, J. R.; Radin, R. L.; Chaudhuri, P.; Pohl, K.; Wieghardt, K.; Nuber, B.; Weiss, J.; Papaefthymiou, G. C.; Frankel, R. B.; Lippard, S. J. *J. Am. Chem. Soc.*, **1987**, *109*, 7387–7396.

Mn–O(bridging)–Mn entity is characterized by Mn–O_b = 2.053 Å, Mn–O_b–Mn = 109.4°, and Mn–Mn = 3.351 Å[36] versus Mn–O_b = 2.155 or 2.206 Å, Mn–O_b–Mn = 112.2 Å, and Mn–Mn = 3.6 Å in $Mn^{II}_3(CH_3CO_2)_6(bpy)_2$. The Mn–$O_b$–Mn system is less "compact" in $Mn^{II}_3(CH_3CO_2)_6(bpy)_2$ than in $[L'_2Mn_2(CH_3CO_2)_2OH]^+$.

Supplementary Material Available: Structure determination details (Table S1), H atom positions (Table S2), anisotropic thermal parameters (Table S3), distances and angles (Table S4) for non-H atoms, and distances and angles (Table S5) for H atoms (8 pages); a listing of structure factors (9 pages). Ordering information is given on any current masthead page.

(36) Bossek, U.; Wieghardt, K.; Nuber, B.; Weiss, J. *Inorg. Chim. Acta* **1989**, *165*, 123–129.

Contribution from the Department of Chemistry, Northern Illinois University, DeKalb, Illinois 60115

Synthesis and Structural Elucidation of Novel Uranyl–Crown Ether Compounds Isolated from Nitric, Hydrochloric, Sulfuric, and Acetic Acids

Robin D. Rogers,* Andrew H. Bond, William G. Hipple, Andrew N. Rollins, and Rodger F. Henry

Received October 16, 1990

The reactions of $UO_2SO_4 \cdot 3H_2O$ with 12-crown-4, 15-crown-5, benzo-15-crown-5, 18-crown-6, and dibenzo-18-crown-6 were investigated in nitric, acetic, hydrochloric, and sulfuric acids. Impurities in the nitric acid resulted in the isolation of the complexes $[(H_5O_2)((NO_2)_2\text{benzo-15-crown-5})_2]_2[(UO_2(NO_3)_2)_2C_2O_4]$ (benzo-15-crown-5 was nitrated during the reaction) and $[(H_3O)(\text{18-crown-6})]_2[(UO_2(NO_3)_2)_2C_2O_4]$, which were crystallographically characterized. $[Mg(OH_2)_6][(H_3O)(\text{15-crown-5})]_2[(UO_2(SO_4))_2C_2O_4]_2$ was also isolated from nitric acid and partially characterized crystallographically. Reactions in acetic acid produced uranyl sulfate polymers with layers of hydrogen-bonded crown ethers in the lattice: $[UO_2(SO_4)(OH_2)_2] \cdot 0.5(\text{12-crown-4}) \cdot H_2O$, $[UO_2(SO_4)(OH_2)_2] \cdot 0.5(\text{benzo-15-crown-5}) \cdot 1.5H_2O$, and $[UO_2(SO_4)(OH_2)_3] \cdot 0.5(\text{18-crown-6})$. Hydronium ion complexes of crown ethers stabilized by $[UO_2Cl_4]^{2-}$ anions were isolated from hydrochloric acid. The complexes $[(H_5O_2)(H_9O_4)(\text{benzo-15-crown-5})_2][UO_2Cl_4]$ and $[(H_5O_2)_2(\text{18-crown-6})][UO_2Cl_4]$ were isolated and crystallographically characterized. Reactions in sulfuric acid for the most part produced decomposition products. $[(H_3O)(\text{dibenzo-18-crown-6})][HSO_4] \cdot CH_3CN$ was isolated by recrystallization of a purple precipitate from CH_3CN/CH_3OH (3:1). $[(H_5O_2)((NO_2)_2\text{benzo-15-crown-5})_2]_2[(UO_2(NO_3)_2)_2C_2O_4]$ crystallizes in the monoclinic space group $P2_1/n$ with (at 22 °C) a = 8.995 (4) Å, b = 19.684 (5) Å, c = 24.739 (4) Å, β = 90.42 (2)°, and D_{calcd} = 1.81 g cm^{-3} for Z = 2 formula units. A final conventional R value of 0.038 was obtained by least-squares refinement with 4790 independent observed reflections [$F_o \geq 5\sigma(F_o)$]. $[(H_3O)(\text{18-crown-6})]_2[(UO_2(NO_3)_2)_2C_2O_4]$ is monoclinic, $P2_1/n$, with (at 22 °C) a = 9.804 (1) Å, b = 21.037 (7) Å, c = 11.827 (3) Å, β = 94.70 (2)°, D_{calcd} = 1.97 g cm^{-3} for Z = 2, and R = 0.040 for 2587 observed reflections. $[UO_2(SO_4)(OH_2)_2] \cdot 0.5(\text{12-crown-4}) \cdot H_2O$ is triclinic, $P\bar{1}$, with (at 22 °C) a = 7.007 (1) Å, b = 8.0408 (6) Å, c = 10.776 (2) Å, α = 91.31 (1)°, β = 93.60 (2)°, γ = 100.18 (1)°, D_{calcd} = 2.83 g cm^{-3}, Z = 2, and R = 0.032 for 1883 observed reflections. $[UO_2(SO_4)(OH_2)_2] \cdot 0.5(\text{benzo-15-crown-5}) \cdot 1.5H_2O$ is triclinic, $P\bar{1}$ with (at 22 °C) a = 6.908 (2) Å, b = 8.717 (4) Å, c = 13.578 (2) Å, α = 79.46 (2)°, β = 75.28 (2)°, γ = 89.98 (3)°, D_{calcd} = 2.41 g cm^{-3}, Z = 2, and R = 0.056 for 2261 observed reflections. $[UO_2(SO_4)(OH_2)_3] \cdot 0.5(\text{18-crown-6})$ is monoclinic, $P2_1/n$, with (at 20 °C) a = 9.314 (5) Å, b = 9.339 (3) Å, c = 16.734 (3) Å, β = 103.62 (3)°, D_{calcd} = 2.59 g cm^{-3} for Z = 4, and R = 0.071 for 1649 observed reflections. $[(H_5O_2)(H_9O_4)(\text{benzo-15-crown-5})_2][UO_2Cl_4]$ is triclinic, $P\bar{1}$, with (at 20 °C) a = 8.889 (3) Å, b = 10.149 (3) Å, c = 11.626 (3) Å, α = 94.54 (2)°, β = 91.04 (2)°, γ = 104.29 (3)°, D_{calcd} = 1.74 g cm^{-3}, Z = 1, and R = 0.034 for 3455 observed reflections. $[(H_5O_2)_2(\text{18-crown-6})][UO_2Cl_4]$ is triclinic, $P\bar{1}$, with (at −150 °C) a = 6.9265 (8) Å, b = 9.239 (1) Å, c = 10.429 (2) Å, α = 93.34 (1)°, β = 103.50 (1)°, γ = 106.15 (1)°, D_{calcd} = 2.02 g cm^{-3}, Z = 1, and R = 0.025 for 2153 observed reflections. $[(H_3O)(\text{dibenzo-18-crown-6})][HSO_4] \cdot CH_3CN$ is triclinic, $P\bar{1}$, with (at 18 °C), a = 9.118 (2) Å, b = 9.348 (5) Å, c = 15.879 (4) Å, α = 77.60 (3)°, β = 80.99 (2)°, γ = 78.22 (3)°, D_{calcd} = 1.34 g cm^{-3}, Z = 2, and R = 0.073 for 1070 observed reflections.

Introduction

Few of the separation studies of the uranyl ion with crown ethers have actually demonstrated metal ion crown ether coordination.[1–13] The probability of the $O{=}U{=}O^{2+}$ ion threading through a crown ether is low. Characterization of uranium complexes is usually limited to dicyclohexyl-18-crown-6 (e.g., $[UO_2(\text{dicyclohexyl-18-crown-6})][ClO_4]_2$:[14] note the use of the poorly coordinating ClO_4^- anion). Other crown ether complexes of uranium that have been structurally characterized include $[U(BH_4)_2(\text{dicyclohexyl-18-crown-6})]_2[UCl_5(BH_4)]$[15] and $[UCl_3(\text{dicyclohexyl-18-crown-6})]_2[UCl_6]$.[16] Inner-sphere complexes have also been reported for several uranium(III) chlorides and crown ethers[17] as well as $[UCl_3(\text{18-crown-6})]$ and $[U(BH_4)_3(\text{18-crown-6})]$.[18]

It is interesting to note the utility ascribed to dicyclohexyl-18-crown-6 and dicyclohexyl-24-crown-8 in uranyl ion extractions. Our structural results with dicyclohexyl-24-crown-8 and other reports in the literature[19–22] for dicyclohexyl-18-crown-6 and dicyclohexyl-24-crown-8 all indicate the presence of hydronium

(1) Brighli, M.; Fux, P.; LaGrange, J.; LaGrange, P. *Inorg. Chem.* **1985**, *24*, 80.
(2) Wang, W.; Chen, B.; Wang, A.; Yu, M.; Liu, X. *He Huax. Yu Fang. Huax.* **1982**, *4*, 139.
(3) Jin, J.; Xu, S.; Liu, M. *He Huax. Yu Fang. Huax.* **1982**, *4*, 147.
(4) Cao, W.; Luo, W. *Yuan. Kex. Jishu* **1987**, *21*, 456.
(5) Deorkar, N. V.; Khopkar, S. M. *J. Radioanal. Nucl. Chem.* **1989**, *130*, 433.
(6) Xu, S.; Jin, J. *He Huax. Yu Fang. Huax.* **1984**, *6*, 232.
(7) Zhang, W.; Xu, S.; Han, Y. *Yuan. Kex. Jishu* **1986**, *20*, 420.
(8) Xu, S.; Zhang, W.; Gu, Z. *Yuan. Kex. Jishu* **1986**, *20*, 425.
(9) Jiang, Y.; Xu, S.; Gu, Z.; Zhang, W. *He Haux. Yu Fang. Huax.* **1982**, *4*, 81.
(10) Wang, W.-J.; Sun, Q.; Chen, B. *J. Radioanal. Nucl. Chem.* **1986**, *98*, 11.
(11) Wang, W.-J.; Sun, Q.; Chen, B. *J. Radioanal. Nucl. Chem.* **1987**, *110*, 227.
(12) Mundra, S. V.; Pai, S. A.; Subramanian, M. S. *J. Radioanal. Nucl. Chem.* **1987**, *116*, 203.
(13) Kojima, T.; Ohno, F.; Fukutomi, H. *Bull. Res. Lab. Nucl. React.* **1981**, *6*, 23.
(14) Navaza, A.; Villain, F.; Charpin, P. *Polyhedron* **1984**, *3*, 143.
(15) Dejean, A.; Charpin, P.; Folcher, G.; Rigny, P.; Navaza, A.; Tsoucaris, G. *Polyhedron* **1987**, *6*, 189.
(16) de Villardi, G. C.; Charpin, P.; Costes, R. M.; Folcher, G.; Plurien, P.; Rigny, P.; deRango, C. *J. Chem. Soc., Chem. Commun.* **1978**, 90.
(17) Hart, F. A.; Tajik, M. *Inorg. Chim. Acta* **1983**, *71*, 169.
(18) Moody, D. C.; Penneman, R. A.; Salazar, K. V. *Inorg. Chem.* **1979**, *18*, 208.
(19) Zheng, P. J.; Wang, M.; Wang, B.; Wu, J.; Wang, W.; Lin, J. *Huax. Xue.* **1988**, *46*, 837.
(20) Wang, W.-J.; Lin, J.; Wang, A.; Zheng, P.; Wang, M.; Wang, B. *Inorg. Chim. Acta* **1988**, *149*, 151.
(21) Wang, W.-J.; Chen, B.; Zheng, P.; Wang, B.; Wang, M. *Inorg. Chim. Acta* **1986**, *117*, 81.
(22) Wang, W.-J.; Jie, L.; Hong, S.; Peiju, Z.; Ming, W.; Boyi, W. *Radiochim. Acta* **1986**, *40*, 199.

0020-1669/91/1330-2671$02.50/0